

Spin-State Gaps and Self-Interaction-Corrected Density Functional Approximations: Octahedral Fe(II) Complexes as Case Study

Selim Romero,¹ Tunna Baruah,² and Rajendra R. Zope²

¹Computational Science Program, The University of Texas at El Paso, El Paso, Texas 79968

²Department of Physics, University of Texas at El Paso, TX, 79968

(Dated: 9 November 2022)

Accurate prediction of spin-state energy difference is crucial for understanding the spin crossover (SCO) phenomena and is very challenging for the density functional approximations, especially for the local and semi-local approximations, due to delocalization errors. Here, we investigate the effect of self-interaction error removal from the local spin density approximation (LSDA) and PBE generalized gradient approximation on the spin-state gaps of Fe(II) complexes with various ligands using recently developed locally scaled self-interaction correction (LSIC) by Zope *et al.* [J. Chem. Phys. **151**, 214108 (2019)]. The LSIC method is exact for one-electron density, recovers uniform electron gas limit of the underlying functional, and approaches the well known Perdew-Zunger self-interaction correction (PZSIC) as a special case when scaling factor is set to unity. Our results, when compared with reference diffusion Monte Carlo (DMC) results, show that PZSIC method significantly overestimates spin-state gaps favoring low spin states for all ligands and does not improve upon DFAs. The perturbative LSIC-LSDA using PZSIC densities significantly improves the gaps with mean absolute error of 0.51 eV but slightly overcorrects for the stronger CO ligands. The quasi self-consistent LSIC-LSDA, like CCSD(T), gives correct sign of spin-state gaps for all ligands with MAE of 0.56 eV, comparable to that of CCSD(T) (0.49 eV).

INTRODUCTION

The Kohn-Sham (KS) formulation of the density functional theory (DFT) is an exact theory that is widely used in many areas, such as chemical physics, materials science, and condensed matter physics¹. Its practical usage requires approximations to the exchange-correlation energy functional, whose complexity determines the accuracy and efficiency of the calculations and system sizes that could be studied. Since there is no systematic way to improve upon the accuracy of exchange-correlation approximations, a large number of density functional approximations (DFAs) with various ingredients have been proposed^{2,3}. Semi-local density functionals, in general, offer a good balance of accuracy and efficiency, hence they are widely used in calculations for large system sizes. While many DFAs perform well for closed-shell systems, they can fail to accurately describe the spin states of the open-shell systems, such as transition metal complexes or organic radicals. Such systems typically have multiple electronic configurations that are close in energy thereby resulting in several accessible spin states. Prototype examples of such systems are spin-crossover Fe-centered complexes⁴⁻³⁵. In these systems, the spin state can change with small variations in temperature. Difficulties of the DFAs in properly describing the *d* electrons in these complexes arise due to inherent self-interaction-error (SIE) in these functionals. SIE can limit their ability to provide qualitatively accurate description of spin-state ordering in these systems.

The SIE in DFA arises due to the incomplete cancellation of

the self-Coulomb energy by the self-exchange energy of the approximate density functionals for one-electron density. The consequences are poor performance for many properties, such as, low reaction barrier heights, underestimation of eigenvalues of valence orbitals, unbound atomic anions, overestimation of polarizabilities of molecular chains, underestimation of band gaps, etc.³⁶⁻⁴⁰ Perdew and coworkers have shown that the density functional total energy of an *N*-electron system should vary linearly between integer numbers of electrons. However, with the approximate density functionals, the total energy of an *N*-electron system varies as a convex curve as the electronic charge varies between *N* and *N* + 1 electrons^{41,42}.

The DFAs artificially lower the energy of a fractional electron system and thereby produce a convex curve instead of a linear curve between integer electron numbers. This deviation from the linearity is often called *delocalization error*⁴³⁻⁴⁶ or sometimes as the *many-electron SIE*⁴⁰. The delocalization error is particularly severe for systems with *d* or *f* electrons. The SIE can result in incorrect charge states and consequently yield erroneous spin state ordering. Indeed, elimination of delocalization errors in the practical density functional calculations is considered as the most outstanding challenge in density functional theory⁴⁷.

In this work, we investigate and compare the effect of one-electron self-interaction correction⁴⁸ (SIC) on the energy gap between spin-states of single Fe-center complexes using recent locally scaled self-interaction correction (LSIC) method of Zope and coworkers⁴⁹ and compare the results with the well-known Perdew-Zunger SIC (PZSIC)⁵⁰ method. The SIC corrections are applied

to the simplest local spin density functional (LSDA) and one of the most widely used generalized-gradient-approximation (GGA) of Perdew-Burke-Ernzerhof (PBE). Our work shows that the PZSIC performs poorly for the spin-state gaps favoring low spin states for all cases while LSIC methods perform significantly better (especially quasi self-consistent LSIC-LSDA) with an mean absolute errors comparable to those of CCSD(T).

In the following Sec. II and III, we provide brief descriptions of the methods used in this work and the computational details. The results and discussion are presented in Sec. IV.

II. THE LOCALLY SCALED SELF-INTERACTION CORRECTION (LSIC METHOD)

LSIC⁴⁹ is a one-electron SIC method, that is, the method is exact for one electron cases, and it employs an orbital-by-orbital correction scheme⁴⁸ in which the total energy is given as

$$E^{LSIC}[\rho_{\uparrow}, \rho_{\downarrow}] = E^{DFA}[\rho_{\uparrow}, \rho_{\downarrow}] + E^{SIC}. \quad (1)$$

Here,

$$E^{SIC} = - \sum_{i\sigma}^{occ} \{U^{LSIC}[\rho_{i\sigma}] + E_{XC}^{LSIC}[\rho_{i\sigma}, 0]\}, \quad (2)$$

with

$$U^{LSIC}[\rho_{i\sigma}] = \frac{1}{2} \int d^3r z_{\sigma}(\vec{r}) \rho_{i\sigma}(\vec{r}) \int d\vec{r}' \frac{\rho_{i\sigma}(\vec{r}')}{|\vec{r} - \vec{r}'|}, \quad (3)$$

$$E_{XC}^{LSIC}[\rho_{i\sigma}, 0] = \int d^3r z_{\sigma}(\vec{r}) \rho_{i\sigma}(\vec{r}) \epsilon_{XC}^{DFA}([\rho_{i\sigma}, 0], \vec{r}), \quad (4)$$

where ϵ_{XC}^{DFA} is the exchange-correlation energy density per particle.

Here, $z_{\sigma}(\vec{r})$ is the local scaling factor $z_{\sigma}(\vec{r}) = \tau_{\sigma}^W(\vec{r})/\tau_{\sigma}(\vec{r})$, where $\tau_{\sigma}^W = |\nabla\rho_{\sigma}|^2/8\rho_{\sigma}$ is the von Weizsäcker kinetic energy density and $\tau_{\sigma}(\vec{r}) = \frac{1}{2}\sum_i |\nabla\psi_{i,\sigma}|^2$ is the non-interacting kinetic energy density.

The scaling factor z_{σ} is an iso orbital indicator which lies between 0 and 1, indicating the nature of the charge for $z_{\sigma}(\vec{r}) = 1$ as single electron density and for $z_{\sigma}(\vec{r}) = 0$ as the uniform electron density. Scaling the self-interaction correction terms with z_{σ} thus retains the full correction for a one-electron density, making the theory exact in that limit, and eliminates the correction in the limit of uniform density where E_{XC}^{DFA} is already exact by design. The LSIC method can be adapted using any suitable iso-orbital indicator similar to the local hybrid functionals.

The well known PZSIC method is a special case of LSIC method when the iso-orbital z_{σ} in Eq. (3) and Eq. (4) is set to 1. The total

energy in LSIC as well in PZSIC depends not only on the density but also on the specific choice of orbitals used to represent that density. Local orbitals are derived from the canonical orbitals through a unitary transformation and the total energy needs to be minimized with respect to the unitary transformation. Both PZSIC and LSIC total energies are evaluated using the Fermi-Löwdin localized orbitals as described in the next section (Sec. II A).

A. Fermi-Löwdin Self-Interaction-Correction

We use LSIC and PZSIC within the Fermi-Löwdin orbital self-interaction correction (FLOSIC) scheme.⁵¹ In the FLOSIC scheme,⁵¹ the SI correction to the total energy in Eq. (2) is computed using local orbitals based on Fermi orbitals (FOs)⁵². The Fermi orbitals are obtained from the spin density matrix and spin density as

$$F_{j\sigma}(\vec{r}) = \frac{\sum_i \psi_{i\sigma}(\vec{a}_{j\sigma}) \psi_{i\sigma}(\vec{r})}{\sqrt{\rho_{\sigma}(\vec{a}_{j\sigma})}}, \quad (5)$$

where i and j are the indices of i^{th} KS orbital and j^{th} FO, respectively, σ is the spin index, and \vec{a}_j are position coordinates referred to as Fermi orbital descriptors (FODs). The FOs are normalized but not orthogonal to each other. Therefore, symmetric orthogonalization is applied to the FOs through the Löwdin⁵³ scheme to obtain Fermi-Löwdin orbitals (FLOs).

The optimal FLOs are obtained by minimizing the E^{PZSIC} with respect to the FOD positions^{54,55} using a gradient optimization scheme⁵⁶. Further details regarding the FLOSIC methodology and examples of FLOSIC calculations for various properties are available in Refs. 51,54,55,57–65.

III. COMPUTATIONAL DETAILS

All of our calculations were performed using the FLOSIC code^{66,67} at the all-electron level and use an extensive Gaussian basis set optimized for the PBE functional.⁶⁸ We note that our results for the PBE functional reproduce the literature results⁵ validating the choice of present of basis sets. The LSDA functional as parameterized in the PW92 functional⁶⁹ is used in the SIC-LSDA calculations. LSIC is well-defined for the LSDA functional with no gauge dependency⁷⁰. Our earlier experience however shows that LSIC often performs well with PBE functional^{70,71} even though the formal gauge dependency occurs. We applied LSIC with both LSDA and PBE functionals in this study. The self-consistent FLOSIC calculations with $z_{\sigma} = 1$, i.e. PZSIC, can be performed either

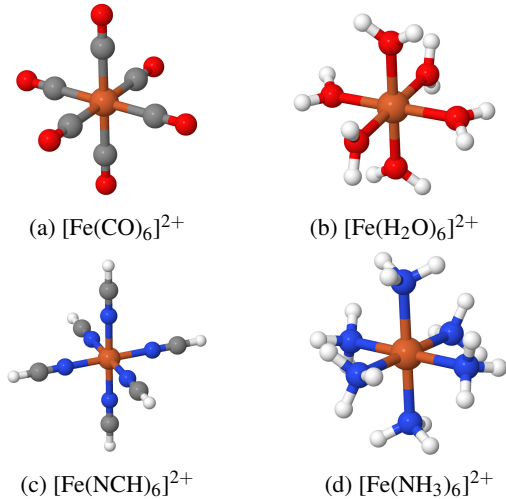


FIG. 1: The molecular structures for the systems $[\text{FeL}_6]^{2+}$ for $L = \text{CO}, \text{H}_2\text{O}, \text{NCH}, \text{and } \text{NH}_3$.

using optimized effective potential within the Krieger-Li-Iafrate approximation⁶¹ or using the Jacobi update approach⁵⁷. Here we used the latter approach. The quasi self-consistent LSIC (qLSIC) calculations are performed by ignoring the variation of scaling factor as explained in Ref. 71. In this approach local scaling is applied to the SIC potential and to the SIC energy density as shown in [Eq. (1)]. We also computed LSIC-DFA total energies using the self-consistent PZSIC densities. A self-consistency tolerance for the total energy of $10^{-6} E_h$ was used in all calculations. The FOD positions were optimized within PZSIC until the forces^{54,55} on the FODs dropped below $10^{-3} E_h/a_0$. All calculations presented herein employed these FOD positions.

Since the self-consistent FLOSIC calculations on the transition metal complexes are not yet very common and are usually challenging, we briefly outline our procedure for reproducibility of our results. To initiate self-consistent FLOSIC calculation, one needs not only an initial guess of density but also an initial set of FODs that are used to construct initial FLOs. In this work we use various initial guesses for the density and FOD sets that are compatible to the initial densities. These initial FOD configurations are generated using our recently developed scheme that generates an FOD structure from any single determinantal wave function. We have generated multiple sets of initial FOD configurations using self-consistent densities from various DFAs for each complex. Additionally, we also begin self-consistent cycle using the superposition of self-interaction-corrected (with LSDA functional) atomic potentials. This procedure usually works. In some cases the self-

interactions-correction can rapidly change the electron density in the self-consistent cycle resulting in non-compatibility between an initial FOD structure (used at the start of self-consistency) and the electron density at a given self-consistent cycle. This breaks the self-consistent FLOSIC cycle due to small eigenvalues of overlap matrix during Löwdin orthogonalization indicating linear dependence of FLOs. This is one of the major difficulties in performing self-consistent FLOSIC calculations. In such cases we use partially self-interaction-corrected densities from previous iteration to generate a new set of FODs and restart the calculations. This procedure can be iterated as needed. The details of this method will be published elsewhere. Starting calculation using multiple initial guesses and FOD configurations resulted in the same final energies for all complexes within the tolerances mentioned in the computational details section. We have included the atomic positions used in this work along with the corresponding final (optimized) set of FOD positions in the supplementary information.

IV. RESULTS AND DISCUSSION

The octahedral Fe(II) complexes studied in this work are shown in Fig. 1. The spin state ordering of such complexes has been studied earlier by a number of groups to examine the performances of various methods in predicting the spin-state gaps.⁴⁻³⁵ We use the complexes studied earlier by Wilbraham and coworkers⁵ at the double-hybrid levels. These complexes are in octahedral conformation with four different ligands (L) where $L = \text{H}_2\text{O}, \text{NH}_3, \text{NCH}, \text{and } \text{CO}$. The ligand field strengths of these four ligands are different. The hexa-aqua and hexa-amine chelated complexes are examples of weak-field limits while the hexa-carbonyl represents a strong field limit. We used the geometries of Wilbraham and coworkers⁵ which are optimized at the PBE0⁷² level of theory, using the modified def2-TZVPP⁷³ large basis set. The valence electronic configuration of Fe is $3d^6 4s^2$. The spin states considered for the Fe(II) complexes are singlet (low spin state) and the quintet (high spin state). In the present calculations the spin-gap between the quintet (HS) and singlet (LS) is defined as

$$\Delta E^{HS-LS} = E(HS) - E(LS). \quad (6)$$

The spin-state gaps defined as ΔE^{HS-LS} are presented for the LSDA, PBE, PZSIC-LSDA, and PZSIC-PBE in Table I. The diffusion Monte-Carlo (DMC) spin-gap energy values from Ref. 14 are taken as reference. For the sake of comparison, coupled-cluster single double and perturbative triple [CCSD(T)] values are also presented. The positive (negative) values in the Table I indicate that the LS (HS) state is more stabilized than HS (LS) state. First, we would like to note that our PBE results are essentially identical to

TABLE I: The spin-state gaps (in eV) calculated with LSDA and PBE functional calculated at the DFA, PZSIC, LSIC, and qLSIC levels. MAEs are with respect to diffusion Monte Carlo (DMC). DMC and CCSD(T) values are from Ref. 5.

System	$[\text{Fe}(\text{H}_2\text{O})_6]^{2+}$	$[\text{Fe}(\text{CO})_6]^{2+}$	$[\text{Fe}(\text{NCH})_6]^{2+}$	$[\text{Fe}(\text{NH}_3)_6]^{2+}$	MAE(eV)
LSDA	-0.49	5.24	2.29	0.98	2.90
PBE	-1.17	3.40	0.96	0.08	1.72
PZSIC-LSDA	1.50	2.11	1.81	2.00	2.75
PZSIC-PBE	1.16	0.93	1.27	1.35	2.08
LSIC-LSDA	-1.26	-0.49	-1.15	-0.82	0.51
LSIC-PBE	-1.06	3.40	-1.02	-0.60	1.08
qLSIC-LSDA	-1.08	0.40	-0.54	-0.50	0.56
qLSIC-PBE	-0.94	4.45	-0.44	-0.34	1.58
CCSD(T)	-1.75	1.33	-0.43	-0.78	0.49
DMC	-1.78	0.59	-1.17	-1.23	

TABLE II: The spin-state gap values (in eV) for $[\text{FeL}_6]^{2+}$ calculated with LSDA and PBE from the DFA part in PZSIC and qLSIC calculations (that is, the first term on right hand side of Eq. (7)). MAEs are computed against DMC. DMC and CCSD(T) reference values are from Ref. 5.

System	$[\text{Fe}(\text{H}_2\text{O})_6]^{2+}$	$[\text{Fe}(\text{CO})_6]^{2+}$	$[\text{Fe}(\text{NCH})_6]^{2+}$	$[\text{Fe}(\text{NH}_3)_6]^{2+}$	MAE(eV)
$\Delta E_{\text{LSDA}}^{\text{PZSIC-LSDA}}$	-1.06	2.55	0.28	-0.17	1.30
$\Delta E_{\text{PBE}}^{\text{PZSIC-LSDA}}$	-1.55	0.93	-0.76	-0.86	0.34
$\Delta E_{\text{LSDA}}^{\text{PZSIC-PBE}}$	-1.08	2.31	0.11	-0.20	1.18
$\Delta E_{\text{PBE}}^{\text{PZSIC-PBE}}$	-1.56	0.69	-0.92	-0.88	0.23
$\Delta E_{\text{LSDA}}^{\text{qLSIC-LSDA}}$	-0.67	4.71	1.69	0.59	2.48
$\Delta E_{\text{PBE}}^{\text{qLSIC-LSDA}}$	-1.29	2.99	0.42	-0.24	1.37
CCSD(T)	-1.75	1.33	-0.43	-0.78	0.49
DMC	-1.78	0.59	-1.17	-1.23	

those of Wilbraham and coworkers⁵ validating our choices of computational parameters and especially of the basis sets. The DFAs, both LSDA and PBE, predict the sign of the spin-state gaps correctly for a weak field ligand H_2O and for a strong field ligand CO . However, the errors for the spin-gaps are rather large, especially for CO . For the other two ligands, both LSDA and PBE favor low spin states. This is generally known^{5,11,12} and has been attributed due to delocalization errors (or self-interaction errors) of these functionals. On the other hand, the Hartree-Fock method which is one electron self-interaction-free and lacks dynamical correlation tend to stabilize high spin states over low spin states. This observation has led to a few studies that explored the reduction of over stabilization by DFAs by mixing various percent of HF exchange in the global hybrid functionals^{5,26,29}. In general, global hybrids functional perform better than the local and semi-local functionals. It has also been noted by Song *et al.* that using HF density in the semi-local

functional results in improved prediction of the spin-state gaps by the semi-local functionals¹⁴. This observation suggests that one-electron self-interaction correction methods such as PZSIC or LSIC might improve spin-gaps.

The spin-state gaps predicted by the PZSIC method are included in Table I. It is evident that PZSIC method does not improve upon the bare DFA functionals except for the CO ligand. The mean absolute errors (MAEs) with LSDA, PBE, PZSIC-LSDA, PZSIC-PBE are 2.90, 1.72, 2.75, and 2.08 eV, respectively. The MAEs show that for the PZSIC-LSDA barely improves LSDA results while for the PBE functional PZSIC performs worse than uncorrected PBE functional. A closer look at the results indicates that PZSIC has a tendency to stabilize the low spin states. Even in the case of a weak field ligand H_2O , where uncorrected LSDA and PBE functionals give qualitatively correct results, the PZSIC favors low spin states thus worsening the DFA spin gap results qualitatively and quanti-

tatively. It has been known that the PZSIC does not improve upon DFAs (especially semi-local DFAs) for thermochemical properties but its performance for spin-state gaps has not been known. This failure of the PZSIC method to predict correct spin states is rather surprising and is the most unexpected result of this work. We will return to the discussion of failure of PZSIC method towards the end of this section.

The scaling down of the SIC in the many-electron regions using the LSIC method brings the results closer to the DMC results (Cf. Table I). This is a perturbative approach that does not change the PZSIC density. The one-shot LSIC method gives results that are in more quantitative agreement with the reference values. The MAE for LSIC-LSDA and LSIC-PBE drops to 0.51 and 1.08 eV from 2.75 and 2.08 eV for PZSIC-LSDA and PZSIC-PBE functionals, respectively. For comparison, the CCSD(T) MAE (0.49 eV) is comparable to LSIC-LSDA MAE. Since one-shot LSIC is a perturbative approach that does not change the PZSIC density, the improvement comes directly from the LSIC energy functional. The perturbative LSIC significantly reduces the excessive SIC correction of the PZSIC thereby improving the results but it slightly overcorrects in case of the strong ligand CO. On the other hand, the quasi-LSIC (qLSIC), where in the orbital dependent SIC potentials are scaled, correctly predicts the sign of spin-state gaps for all the complexes studied here. The MAE of the spin-gaps in the case of qLSIC-LSDA is 0.56 eV which is comparable to that of CCSD(T) (0.49 eV). The results also show that both qLSIC and one shot LSIC perform better with the simpler LSDA than with the PBE functional.

To understand the improved performance of the LSIC method and the failure of PZSIC method, we analyze the contributions to the spin-state gap from the DFA energy terms, i.e., the first term on the right hand side (RHS) of Eq. (1), and the sum of orbitalwise SIC corrections (i.e., Eq. (2)). Thus we substitute Eq.(1) into the Eq. (6) resulting in the following expression.

$$\Delta E^{HS-LS} = \Delta E_{DFA}^{HS-LS} + \Delta E_{SIC}^{HS-LS}. \quad (7)$$

The first term on the RHS is therefore the DFA spin-state gap evaluated using the SIC density and the second term is the correction due to the energy. This analysis, in some sense, is similar to the HF-DFT approach⁷⁴⁻⁷⁷. Unlike the HF-DFT however, the advantage here is that the E^{DFA} contributions are part of the PZSIC and qLSIC energies and no additional calculations are required.

The DFA contribution to the spin-state gaps calculated on self-consistent PZSIC-DFA and qLSIC-DFA densities are shown in Table II. To simplify the discussion below we use ΔE_{En}^{Den} notation to convey the calculation scheme where the subscript refers to the energy functional and the superscript refers to the underlying functional for the SIC density. The MAE of $\Delta E_{LSDA}^{PZSIC-LSDA}$ is 1.30 eV. This is significantly better than that of LSDA (MAE = 2.90 eV).

Thus, the density changes due to SIC (to the potential) within the PZSIC method result in reduction of MAE by about 1.6 eV. Even more spectacular reduction in error is obtained in case of PBE functional. The $\Delta E_{PBE}^{PZSIC-PBE}$ has MAE of only 0.23 eV in contrast to 2.08 eV of of PZSIC-PBE. This is half the MAE of the CCSD(T) method (0.49 eV). As all self-consistent calculations performed with SIC methods herein generate *self-interaction free* densities, we can use these SIC densities in uncorrected DFAs used in this work to get some idea about error cancellations that play role in predicting spin-state gaps. It turns out that the PBE functional performs excellently not only with the PZSIC-PBE density but also with PZSIC-LSDA densities (with MAE = 0.34 eV). This suggests that more sophisticated meta-GGA functionals may also perform well for spin-state gaps but that discussion is beyond the scope of present work. The use of qLSIC densities in the uncorrected DFAs however do not show similar level of improvement in the spin state gaps. For example, the $\Delta E_{LSDA}^{qLSIC-LSDA}$ has an MAE of 2.48 eV which is comparable to that of LSDA. Similarly, the $\Delta E_{PBE}^{qLSIC-PBE}$ has an MAE of 1.37 eV. These results are not very surprising. It is apparent from Eq. (7) that any method that performs well with ΔE_{DFA}^{HS-LS} for spin-state gaps must yield a small contribution from the SIC term (ΔE_{SIC}^{HS-LS}). This gives a hint that a poor performance of PZSIC is therefore due to its excessive SIC to the energy. Indeed such a tendency of PZSIC to excessively correct has also been seen in earlier studies.^{49,60,71,78} This excessive correcting tendency of PZSIC results in somewhat greater localization of density which might be beneficial for use in uncorrected DFAs for removing delocalization errors as done in the HF-DFT or density corrected DFT and also seen in the present results. As discussed below, among all the self-consistent SIC methods used here the PZSIC density is the most localized. The density differences between the PZSIC and LSDA, and between qLSIC and LSDA are plotted in Fig. 2 for $\text{Fe}(\text{NCH})_6^{2+}$. The red isosurface shows the regions where DFA density is larger than the qLSIC/PZSIC density. The LSDA density is higher in the interatomic region around the Fe center compared to the SIC density. This plot also shows that although the density differences with PZSIC and qLSIC are similar, with qLSIC the differences are smaller particularly near the Fe center. To obtain additional evidence about the (greater) localizing tendency of PZSIC, we compute the spin charges at Fe(II) in the complex by integrating the spin densities within atomic spheres centered at Fe and with radius equal to van der Wall radius of Fe. Likewise, we also compute spin charges using Löwdin's population analysis. These results are presented in Table III. It is evident from the the table that the uncorrected LSDA and PBE functionals have the smallest values of spin charges consistent with a known delocalization of density within these methods. On the other hand, PZSIC has the largest values of spin charges among

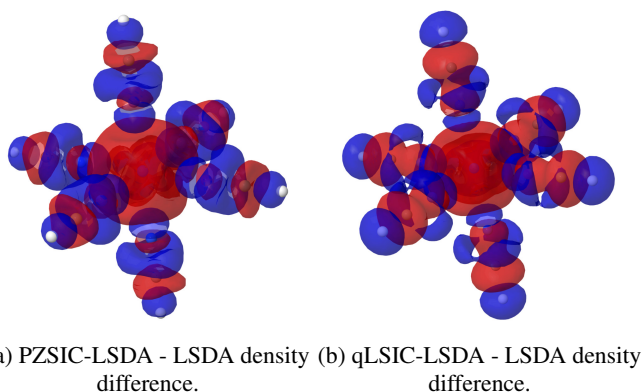


FIG. 2: Total density difference of (a) PZSIC-LSDA and LSDA and (b) qLSIC-LSDA and LSDA for the $[\text{Fe}(\text{NCH})_6]^{2+}$ complex in the LS state. The isosurface value used for both images is $0.0005e$ and the red (blue) surface shows regions where LSDA density is larger (smaller).

all methods suggesting its spin density to be most localized amongst all methods. This is consistent with above discussion. On the other hand, the qLSIC spin charges are intermediate between the PZSIC and uncorrected DFA spin charges. The less localized qLSIC density is not favorable for use in uncorrected DFAs for the density corrected DFT calculations. The qLSIC-LSDA provides most balanced description of the spin-state gaps [comparable to CCSD(T)] where in both the terms in Eq. (6) contribute to the gap. The qLSIC-LSDA also predicts the correct sign for spin-state gaps for all ligands. The qLSIC-PBE doesn't perform as well as qLSIC-LSDA possibly due to gauge-dependence⁷⁰.

V. CONCLUSIONS

In summary, we have examined the effect of SIC on the spin-state gaps of octahedral $[\text{Fe}(\text{II})\text{L}_6]^{2+}$ complexes with $\text{L}=\text{CO}$, NCH , NH_3 , and H_2O using the LSIC and PZSIC methods. One surprising result is that the PZSIC fails to improve upon the DFA results for weak field ligands and has a propensity to stabilize low spin states. Analysis of results show that the PZSIC energy functional provides too much SI correction to the energy. In fact, no PZSIC energy correction is needed as DFA part of PZSIC functional alone is sufficient to provide good spin-gaps. The analysis of results show that the self- PZSIC produces more localized density than the quasi-self-consistent LSIC method. The more localized density is favorable for use in uncorrected functional as in the HF-DFT or density cor-

rected DFT. Indeed the spin-state gaps obtained using DFA functional on PZSIC densities are significantly improved compared to those of self-consistent PZSIC or DFA results. This improvement is spectacular for the PBE functional. The perturbative LSIC results evaluated on the PZSIC densities predicts accurate spin-state gaps and its performance is comparable to that of CCSD(T) method even with the simplest DFA. Likewise, qLSIC-LSDA predicts correct sign for spin-gaps for all ligands with mean absolute error comparable to that of CCSD(T). LSIC does not work that well with PBE functional especially for the CO ligand possibly due to gauge dependency. Still, it is very gratifying that the simplest (LSDA) density functional when corrected for SIE using the LSIC method, accurately predicts spin-state gaps of Fe(II) complexes and predicts correct spin states as most stable states. It remains unclear if the LSIC method will perform to the same degree of excellence for other SCO complexes. We will be undertaking a large scale study to address this question.

DATA AVAILABILITY STATEMENT

The data that supports the findings of this study are available within the article.

ACKNOWLEDGMENTS

Authors acknowledge Dr. Yoh Yamamoto for discussions. This work was supported by the US Department of Energy, Office of Science, Office of Basic Energy Sciences, as part of the Computational Chemical Sciences Program under Award No. DE-SC0018331. Support for computational time at the Texas Advanced Computing Center and at NERSC is gratefully acknowledged. SR expresses his gratitude to the Mexican National Council for Science and Technology (CONACYT) for financial support.

¹R. O. Jones, "Density functional theory: Its origins, rise to prominence, and future," *Rev. Mod. Phys.* **87**, 897 (2015).

²J. P. Perdew and K. Schmidt, "Jacob's ladder of density functional approximations for the exchange-correlation energy," *AIP Conf. Proc.* **577**, 1–20 (2001), <https://aip.scitation.org/doi/pdf/10.1063/1.1390175>.

³M. A. Marques, M. J. Oliveira, and T. Burnus, "Libxc: A library of exchange and correlation functionals for density functional theory," *Comput. Phys. Commun.* **183**, 2272–2281 (2012).

⁴Y. Cytter, A. Nandy, A. Bajaj, and H. J. Kulik, "Ligand additivity and divergent trends in two types of delocalization errors from approximate density functional theory," *J. Chem. Phys.* **13**, 4549–4555 (2022).

⁵L. Wilbraham, C. Adamo, and I. Ciofini, "Communication: Evaluating non-empirical double hybrid functionals for spin-state energetics in transition-metal complexes," *J. Chem. Phys.* **148**, 041103 (2018), <https://doi.org/10.1063/1.5019641>.

TABLE III: Spin charges (in e) at the Fe site for the high spin state in various approximations. Spin charges are obtained from Löwdin population analysis and by integrating spin density using atomic sphere (see text for details).

Population analysis	H ₂ O				CO			
	LSDA		PBE		LSDA		PBE	
	Atomic sphere	Löwdin	Atomic sphere	Löwdin	Atomic sphere	Löwdin	Atomic sphere	Löwdin
DFA	3.607	3.648	3.637	3.674	3.509	3.665	3.554	3.695
PZSIC	3.768	3.799	3.764	3.793	3.734	3.792	3.708	3.797
qLSIC	3.686	3.724	3.703	3.737	3.587	3.715	3.608	3.727

⁶M. Radoń, “Benchmarking quantum chemistry methods for spin-state energetics of iron complexes against quantitative experimental data,” *Phys. Chem. Chem. Phys.* **21**, 4854–4870 (2019).

⁷H. J. Kulik, “Making machine learning a useful tool in the accelerated discovery of transition metal complexes,” *WIREs Comput. Mol. Sci.* **10**, e1439 (2020).

⁸A. Nandy, D. B. Chu, D. R. Harper, C. Duan, N. Arunachalam, Y. Cytter, and H. J. Kulik, “Large-scale comparison of 3d and 4d transition metal complexes illuminates the reduced effect of exchange on second-row spin-state energetics,” *Phys. Chem. Chem. Phys.* **22**, 19326–19341 (2020).

⁹M. Alipour and T. Izadkhast, “Appraising spin-state energetics in transition metal complexes using double-hybrid models: accountability of SOS0-PBESCAN0-2 (a) as a promising paradigm,” *Phys. Chem. Chem. Phys.* **22**, 9388–9404 (2020).

¹⁰S. Vela, M. Fumanal, J. Cirera, and J. Ribas-Arino, “Thermal spin crossover in Fe(II) and Fe(III): accurate spin state energetics at the solid state,” *Phys. Chem. Chem. Phys.* **22**, 4938–4945 (2020).

¹¹L. A. Mariano, B. Vlasisavljević, and R. Poloni, “Biased spin-state energetics of Fe(II) molecular complexes within density-functional theory and the linear-response hubbard U correction,” *J. Chem. Theory Comput.* **16**, 6755–6762 (2020).

¹²L. A. Mariano, B. Vlasisavljević, and R. Poloni, “Improved Spin-State Energy Differences of Fe(II) molecular and crystalline complexes via the Hubbard U-corrected density,” *J. Chem. Theory Comput.* **17**, 2807–2816 (2021).

¹³B. M. , Flöser, Y. Guo, C. Riplinger, F. Tuczek, and F. Neese, “Detailed pair natural orbital-based coupled cluster studies of spin crossover energetics,” *J. Chem. Theory Comput.* **16**, 2224–2235 (2020).

¹⁴S. Song, M.-C. Kim, E. Sim, A. Benali, O. Heinonen, and K. Burke, “Benchmarks and reliable DFT results for spin gaps of small ligand Fe(II) complexes,” *J. Chem. Theory Comput.* **14**, 2304–2311 (2018).

¹⁵A. Patra, H. Peng, J. Sun, and J. P. Perdew, “Rethinking co adsorption on transition-metal surfaces: Effect of density-driven self-interaction errors,” *Phys. Rev. B* **100**, 035442 (2019).

¹⁶A. Droghetti, D. Alfè, and S. Sanvito, “Assessment of density functional theory for iron (II) molecules across the spin-crossover transition,” *J. Chem. Phys.* **137**, 124303 (2012).

¹⁷G. Ganzenmüller, N. Berkaïne, A. Fouqueau, M. E. Casida, and M. Reiher, “Comparison of density functionals for differences between the high-⁽⁵⁾T_{2g} and low-⁽¹⁾A_{1g} spin states of iron (II) compounds. IV. Results for the ferrous complexes [Fe(L)(‘NHS 4’)],” *J. Chem. Phys.* **122**, 234321 (2005).

¹⁸D. N. Bowman and E. Jakubikova, “Low-spin versus high-spin ground state in pseudo-octahedral iron complexes,” *Inorg. Chem.* **51**, 6011–6019 (2012).

¹⁹A. Fouqueau, S. Mer, M. E. Casida, L. M. Lawson Daku, A. Hauser, T. Mineva, and F. Neese, “Comparison of density functionals for energy and structural differences between the high-⁽⁵⁾T_{2g}:(t_{2g})⁴(eg)² and low-⁽¹⁾A_{1g}:(t_{2g})⁶(eg)⁰ spin states of the hexaquoferrous cation [Fe(H₂O)₆]²⁺,” *J. Chem. Phys.* **120**, 9473–9486 (2004).

²⁰A. Fouqueau, M. E. Casida, L. M. L. Daku, A. Hauser, and F. Neese, “Comparison of density functionals for energy and structural differences between the high-⁽⁵⁾T_{2g}:(t_{2g})⁴(eg)² and low-⁽¹⁾A_{1g}:(t_{2g})⁶(eg)⁰ spin states of iron (II) coordination compounds. II. more functionals and the hexaminoferrous cation, [Fe(NH₃)₆]²⁺,” *J. Chem. Phys.* **122**, 044110 (2005).

²¹K. Pierloot and S. Vancoillie, “Relative energy of the high-⁽⁵⁾T_{2g} and low-⁽¹⁾A_{1g} spin states of [Fe(H₂O)₆]²⁺, [Fe(NH₃)₆]²⁺, and [Fe(bpy)₃]²⁺: CASPT2 versus density functional theory,” *J. Chem. Phys.* **125**, 124303 (2006).

²²K. Pierloot and S. Vancoillie, “Relative energy of the high-⁽⁵⁾T_{2g} and low-⁽¹⁾A_{1g} spin states of the ferrous complexes [Fe(L)(NHS₄)]: CASPT2 versus density functional theory,” *J. Chem. Phys.* **128**, 034104 (2008).

²³L. Wilbraham, P. Verma, D. G. Truhlar, L. Gagliardi, and I. Ciofini, “Multiconfiguration pair-density functional theory predicts spin-state ordering in iron complexes with the same accuracy as complete active space second-order perturbation theory at a significantly reduced computational cost,” *J. Phys. Chem. Lett.* **8**, 2026–2030 (2017).

²⁴P. Verma, Z. Varga, J. E. Klein, C. J. Cramer, L. Que, and D. G. Truhlar, “Assessment of electronic structure methods for the determination of the ground spin states of Fe(II), Fe(III) and Fe(IV) complexes,” *Phys. Chem. Chem. Phys.* **19**, 13049–13069 (2017).

²⁵S. Ye and F. Neese, “Accurate modeling of spin-state energetics in spin-crossover systems with modern density functional theory,” *Inorg. Chem.* **49**, 772–774 (2010).

²⁶E. I. Ioannidis and H. J. Kulik, “Towards quantifying the role of exact exchange in predictions of transition metal complex properties,” *J. Chem. Phys.* **143**, 034104 (2015).

²⁷A. Rudavskiy, C. Sousa, C. de Graaf, R. W. Havenith, and R. Broer, “Computational approach to the study of thermal spin crossover phenomena,” *J. Chem. Phys.* **140**, 184318 (2014).

²⁸M. Fumanal, L. K. Wagner, S. Sanvito, and A. Droghetti, “Diffusion monte carlo perspective on the spin-state energetics of [Fe(NCH)₆]²⁺,” *J. Chem. Theory Comput.* **12**, 4233–4241 (2016), pMID: 27500854, <https://doi.org/10.1021/acs.jctc.6b00332>.

²⁹B. Pinter, A. Chankisijjev, P. Geerlings, J. N. Harvey, and F. De Proft, “Conceptual insights into DFT spin-state energetics of octahedral transition-metal complexes through a density difference analysis,” *Chem. Eur. J.* **24**, 5281–5292 (2018).

³⁰S. R. Mortensen and K. P. Kepp, “Spin propensities of octahedral complexes from density functional theory,” *J. Phys. Chem. A* **119**, 4041–4050 (2015).

³¹L. M. Lawson Daku, F. Aquilante, T. W. Robinson, and A. Hauser, “Accurate spin-state energetics of transition metal complexes. I. CCSD(T), CASPT2, and DFT study of [M(NCH)₆]²⁺ (M= Fe, Co),” *J. Chem. Theory Comput.* **8**, 4216–4231 (2012).

³²M. Kepenekian, V. Robert, B. Le Guennic, and C. De Graaf, “Energetics of [Fe(NCH)₆]²⁺ via CASPT2 calculations: A spin-crossover perspective,” *J. Comput. Chem.* **30**, 2327–2333 (2009).

- ³³A. Domingo, M. Àngels Carvajal, and C. De Graaf, "Spin crossover in Fe(II) complexes: An ab initio study of ligand σ -donation," *Int. J. Quantum Chem.* **110**, 331–337 (2010).
- ³⁴B. G. Janesko, "Reducing density-driven error without exact exchange," *Phys. Chem. Chem. Phys.* **19**, 4793–4801 (2017).
- ³⁵M. Swart, "Accurate spin-state energies for iron complexes," *J. Chem. Theory Comput.* **4**, 2057–2066 (2008).
- ³⁶J. P. Perdew, "Accurate density functional for the energy: Real-space cutoff of the gradient expansion for the exchange hole," *Phys. Rev. Lett.* **55**, 2370–2370 (1985).
- ³⁷L. J. Sham and M. Schlüter, "Density-functional theory of the energy gap," *Phys. Rev. Lett.* **51**, 1888–1891 (1983).
- ³⁸S. Patchkovskii and T. Ziegler, "Improving "difficult" reaction barriers with self-interaction corrected density functional theory," *J. Chem. Phys.* **116**, 7806–7813 (2002), <https://doi.org/10.1063/1.1468640>.
- ³⁹J. Gräfenstein, E. Kraka, and D. Cremer, "The impact of the self-interaction error on the density functional theory description of dissociating radical cations: Ionic and covalent dissociation limits," *J. Chem. Phys.* **120**, 524–539 (2004), <https://doi.org/10.1063/1.1630017>.
- ⁴⁰A. Ruzsinszky, J. P. Perdew, G. I. Csonka, O. A. Vydrov, and G. E. Scuseria, "Spurious fractional charge on dissociated atoms: Pervasive and resilient self-interaction error of common density functionals," *J. Chem. Phys.* **125**, 194112 (2006), <https://doi.org/10.1063/1.2387954>.
- ⁴¹P. Mori-Sánchez, A. J. Cohen, and W. Yang, "Localization and delocalization errors in density functional theory and implications for band-gap prediction," *Phys. Rev. Lett.* **100**, 146401 (2008).
- ⁴²A. J. Cohen, P. Mori-Sánchez, and W. Yang, "Insights into current limitations of density functional theory," *Science* **321**, 792–794 (2008), <https://www.science.org/doi/pdf/10.1126/science.1158722>.
- ⁴³X. Zheng, M. Liu, E. R. Johnson, J. Contreras-García, and W. Yang, "Delocalization error of density-functional approximations: A distinct manifestation in hydrogen molecular chains," *J. Chem. Phys.* **137**, 214106 (2012), <https://doi.org/10.1063/1.4768673>.
- ⁴⁴A. D. Dwyer and D. J. Tozer, "Dispersion, static correlation, and delocalisation errors in density functional theory: An electrostatic theorem perspective," *J. Chem. Phys.* **135** (2011), [10.1063/1.3653980](https://doi.org/10.1063/1.3653980).
- ⁴⁵C. Li, X. Zheng, N. Q. Su, and W. Yang, "Localized orbital scaling correction for systematic elimination of delocalization error in density functional approximations," *Natl. Sci. Rev.* **5**, 203–215 (2018).
- ⁴⁶E. R. Johnson, A. Otero-de-la Roza, and S. G. Dale, "Extreme density-driven delocalization error for a model solvated-electron system," *J. Chem. Phys.* **139**, 184116 (2013), <https://doi.org/10.1063/1.4829642>.
- ⁴⁷K. R. Bryenton, A. A. Adeleke, S. G. Dale, and E. R. Johnson, "Delocalization error: The greatest outstanding challenge in density-functional theory," *WIREs Comput. Mol. Sci.* **10**, 1002/wcms.1631.
- ⁴⁸I. Lindgren, "A statistical exchange approximation for localized electrons," *Int. J. Quantum Chem.* **5**, 411–420 (1971).
- ⁴⁹R. R. Zope, Y. Yamamoto, C. M. Diaz, T. Baruah, J. E. Peralta, K. A. Jackson, B. Santra, and J. P. Perdew, "A step in the direction of resolving the paradox of Perdew-Zunger self-interaction correction," *J. Chem. Phys.* **151**, 214108 (2019), <https://doi.org/10.1063/1.5129533>.
- ⁵⁰J. P. Perdew and A. Zunger, "Self-interaction correction to density-functional approximations for many-electron systems," *Phys. Rev. B* **23**, 5048–5079 (1981).
- ⁵¹M. R. Pederson, A. Ruzsinszky, and J. P. Perdew, "Communication: Self-interaction correction with unitary invariance in density functional theory," *J. Chem. Phys.* **140**, 121103 (2014), <https://doi.org/10.1063/1.4869581>.
- ⁵²W. L. Luken and D. N. Beratan, "Localized orbitals and the Fermi hole," *Theoret. Chim. Acta* **61**, 265–281 (1982).
- ⁵³P.-O. Löwdin, "On the non-orthogonality problem connected with the use of atomic wave functions in the theory of molecules and crystals," *J. Chem. Phys.* **18**, 365–375 (1950), <https://doi.org/10.1063/1.1747632>.
- ⁵⁴M. R. Pederson, "Fermi orbital derivatives in self-interaction corrected density functional theory: Applications to closed shell atoms," *J. Chem. Phys.* **142**, 064112 (2015), <https://doi.org/10.1063/1.4907592>.
- ⁵⁵M. R. Pederson and T. Baruah, "Chapter eight - self-interaction corrections within the fermi-orbital-based formalism," in *Advances In Atomic, Molecular, and Optical Physics*, Vol. 64, edited by E. Arimondo, C. C. Lin, and S. F. Yelin (Academic Press, 2015) pp. 153–180.
- ⁵⁶D. C. Liu and J. Nocedal, "On the limited memory BFGS method for large scale optimization," *Math. Program.* **45**, 503–528 (1989).
- ⁵⁷Z.-h. Yang, M. R. Pederson, and J. P. Perdew, "Full self-consistency in the fermi-orbital self-interaction correction," *Phys. Rev. A* **95**, 052505 (2017).
- ⁵⁸M. R. Pederson, T. Baruah, D.-y. Kao, and L. Basurto, "Self-interaction corrections applied to mg-porphyrin, c60, and pentacene molecules," *J. Chem. Phys.* **144**, 164117 (2016), <https://doi.org/10.1063/1.4947042>.
- ⁵⁹S. Schwalbe, T. Hahn, S. Liebing, K. Trepte, and J. Kortus, "Fermi-Löwdin orbital self-interaction corrected density functional theory: Ionization potentials and enthalpies of formation," *J. Comput. Chem.* **39**, 2463–2471 (2018), <https://onlinelibrary.wiley.com/doi/pdf/10.1002/jcc.25586>.
- ⁶⁰Y. Yamamoto, C. M. Diaz, L. Basurto, K. A. Jackson, T. Baruah, and R. R. Zope, "Fermi-Löwdin orbital self-interaction correction using the strongly constrained and appropriately normed meta-GGA functional," *J. Chem. Phys.* **151**, 154105 (2019), <https://doi.org/10.1063/1.5120532>.
- ⁶¹C. M. Diaz, T. Baruah, and R. R. Zope, "Fermi-löwdin-orbital self-interaction correction using the optimized-effective-potential method within the Krieger-Li-Iafrate approximation," *Phys. Rev. A* **103**, 042811 (2021).
- ⁶²C. M. Diaz, L. Basurto, S. Adhikari, Y. Yamamoto, A. Ruzsinszky, T. Baruah, and R. R. Zope, "Self-interaction-corrected Kohn-Sham effective potentials using the density-consistent effective potential method," *J. Chem. Phys.* **155**, 064109 (2021), <https://doi.org/10.1063/5.0056561>.
- ⁶³F. W. Aquino, R. Shinde, and B. M. Wong, "Fractional occupation numbers and self-interaction correction-scaling methods with the Fermi-Löwdin orbital self-interaction correction approach," *J. Comput. Chem.* **41**, 1200–1208 (2020), <https://onlinelibrary.wiley.com/doi/pdf/10.1002/jcc.26168>.
- ⁶⁴P. Mishra, Y. Yamamoto, J. K. Johnson, K. A. Jackson, R. R. Zope, and T. Baruah, "Study of self-interaction-errors in barrier heights using locally scaled and Perdew-Zunger self-interaction methods," *J. Chem. Phys.* **156**, 014306 (2022), <https://doi.org/10.1063/5.0070893>.
- ⁶⁵P. Mishra, Y. Yamamoto, P.-H. Chang, D. B. Nguyen, J. E. Peralta, T. Baruah, and R. R. Zope, "Study of self-interaction errors in density functional calculations of magnetic exchange coupling constants using three self-interaction correction methods," *J. Phys. Chem. A* **126**, 1923–1935 (2022), PMID: 35302373, <https://doi.org/10.1021/acs.jpca.1c10354>.
- ⁶⁶R. R. Zope, T. Baruah, and K. A. Jackson, "FLOSIC 0.2," Based on the NRLMOL code of M. R. Pederson.
- ⁶⁷Y. Yamamoto, L. Basurto, C. M. Diaz, R. R. Zope, and T. Baruah, "Self-interaction correction to density functional approximations using Fermi-Löwdin orbitals: methodology and parallelization," Unpublished.
- ⁶⁸D. Porezag and M. R. Pederson, "Optimization of Gaussian basis sets for density-functional calculations," *Phys. Rev. A* **60**, 2840–2847 (1999).
- ⁶⁹J. P. Perdew and Y. Wang, "Accurate and simple analytic representation of the electron-gas correlation energy," *Phys. Rev. B* **45**, 13244–13249 (1992).
- ⁷⁰P. Bhattarai, K. Wagle, C. Shahi, Y. Yamamoto, S. Romero, B. Santra, R. R. Zope, J. E. Peralta, K. A. Jackson, and J. P. Perdew, "A step in the direction of resolving the paradox of Perdew-Zunger self-interaction correction. II. gauge consistency of the energy density at three levels of approximation," *J. Chem. Phys.* **152**, 214109

- (2020), <https://doi.org/10.1063/5.0010375>.
- ⁷¹S. Akter, Y. Yamamoto, C. M. Diaz, K. A. Jackson, R. R. Zope, and T. Baruah, "Study of self-interaction errors in density functional predictions of dipole polarizabilities and ionization energies of water clusters using Perdew-Zunger and locally scaled self-interaction corrected methods," *J. Chem. Phys.* **153**, 164304 (2020), <https://doi.org/10.1063/5.0025601>.
- ⁷²C. Adamo and V. Barone, "Toward reliable density functional methods without adjustable parameters: The PBE0 model," *J. Chem. Phys.* **110**, 6158–6170 (1999), <https://doi.org/10.1063/1.478522>.
- ⁷³F. Weigend, "Accurate coulomb-fitting basis sets for H to Rn," *Phys. Chem. Chem. Phys.* **8**, 1057–1065 (2006).
- ⁷⁴P. Verma, A. Perera, and R. J. Bartlett, "Increasing the applicability of DFT I: Non-variational correlation corrections from Hartree-Fock DFT for predicting transition states," *Chem. Phys. Lett.* **524**, 10–15 (2012).
- ⁷⁵M.-C. Kim, E. Sim, and K. Burke, "Understanding and reducing errors in density functional calculations," *Phys. Rev. Lett.* **111**, 073003 (2013).
- ⁷⁶S. Vuckovic, S. Song, J. Kozłowski, E. Sim, and K. Burke, "Density functional analysis: the theory of density-corrected DFT," *J. Chem. Theory Comput.* **15**, 6636–6646 (2019).
- ⁷⁷B. G. Janesko, "Replacing hybrid density functional theory: motivation and recent advances," *Chem. Soc. Rev.* (2021).
- ⁷⁸O. A. Vydrov and G. E. Scuseria, "Effect of the Perdew-Zunger self-interaction correction on the thermochemical performance of approximate density functionals," *J. Chem. Phys.* **121**, 8187–8193 (2004), <https://aip.scitation.org/doi/pdf/10.1063/1.1794633>.